

Neural Data Exploration with Force Feedback

Laura Raya¹, Miguel A. Otaduy¹ and Marcos García¹

¹Grupo de Modelado y Realidad Virtual (GMRV), Rey Juan Carlos University (URJC), Madrid

Abstract

The behavior of the brain depends to a large extent on its neural structure. Therefore, understanding this neural topology is a high-priority research line for neurobiologists. Due to complexity of the brain's neural structure, visual representations look tangled, and extracting knowledge from them is a difficult task. In this work, we propose the use of multimodal interfaces to enhance neurobiologists' understanding of neural data. Our system is based on four pillars: a stereo rendering module, a camera control system, a visual aid unit, and a haptically constrained navigation tool. We observe that haptically aided navigation helps neurobiologists analyze the brain's topology. Our system uses stylus-based haptic devices with two purposes: they provide a natural interface to deal with 3D data (controlling camera motion) and they constrain the user's motion. The system was built trying to keep user interactions as intuitive as possible.

Categories and Subject Descriptors (according to ACM CCS): I.3.4 [Computer Graphics]: Graphics Utilities—Virtual device interfaces. I.3.8 [Computer Graphics]: Applications—. H.5.2 [Information Interfaces and presentation]: User Interfaces—Haptic.

1. Introduction

Research on the human brain can be tremendously useful to prevent or cure several diseases. However, the brain's complexity makes its understanding challenging, specially when it comes to the study of neural structures and their topology. A typical neuron is composed of a cell body (often called the soma), dendrites, and an axon. Dendrites are filaments that arise from the cell body, often extending for hundreds of micrometers and branching multiple times, giving rise to a complex tree.

Nowadays, there is a growing interest in biologically detailed brain visualization [Mar06]. There are several scientific applications and innovative visualization techniques aimed at helping neuroscientists and biologists in the study of neural network structures and their performance [KRH*06, MMYK06, LHH*]. However, these visualization techniques exploit only the visual modality. Various researchers have shown that the use of multiple sensory modalities can help the execution of different tasks and the interpretation of large and complex datasets [BOYBK]. In the case of neural structures, haptic guidance along the different neurons might facilitate the monitoring of individual dendrites or axons. Helping the user to follow segments or complex geometric surfaces has already been investigated in

the past [TKCM, GL09]. The existing techniques do not perform well in complex branching situations. We use a constrained gradient-descent algorithm to facilitate navigation in such cases as in the case of neural networks.

When the user navigates in complex environments with multiple small structures, these may be occluded by other structures, complicating path selection. Stereo vision can enhance visualization and helps in the analysis of complex three-dimensional environments [KK10].

In this paper, we present a multimodal interface to navigate along segmented neural structures. Our main goal is to help neurobiologists understand the topology of neural data through a multimodal navigation system. Our system is based on four pillars: a stereo render module, a camera control system, a visual aids unit, and a haptic navigation module to navigate along the filiform structure, by constraining motion.

2. Navigation System

This section describes the four main modules of our navigation system: stereo vision, camera control, visual aids, and haptic navigation.

2.1. Stereo Vision Module

When projecting filiform structures over the screen, it is easy to lose depth perception. A stereo-render module has been implemented to incorporate the stereo fusion effect as an additional depth cue (Fig. 1). Currently, our stereo module works on an ARvision-3D HMD device (Fig. 3) and it can be enabled or disabled by users.

Our stereo system is designed for head mounted displays (HMDs). A stereo image consists of two fields which display only its corresponding eye. Two different virtual cameras are used to render both fields. These cameras are separated by an inter-ocular distance IOD . An HMD renders the two stereo fields on different screens, so the two cameras have the same symmetric frustum.

When the inter-ocular distance IOD increases, the absolute magnitude of both positive and negative parallax values increase, causing, in some cases, an increase in depth perception. However, large positive parallax values complicate the fusion of the two stereo fields. We have stressed the perspective by increasing the camera's horizontal projection angle improves user's sensation (Fig. 1). It allows smaller inter-ocular distances, making image fusion easier.

Our system allows two different inter-ocular configurations: static and dynamic. In the static configuration, the IOD is preset by the user. During navigation, the IOD is fixed and the positive parallax increases when the user moves toward the scene. This behavior is consistent with the real world and it is used in augmented reality. However, the increase in positive parallax might cause fusion error. In the dynamic configuration, parallax is controlled during navigation, by keeping the relative distance to the center of the workspace constant. This method computes the IOD value as a factor of the dynamic distance d between the camera and the center of the virtual workspace: $IOD = d * 0.065 / D$. D indicates a reference distance to the center of the workspace, and 0.065 is the mean human inter-ocular distance (i.e. 6.5cm).

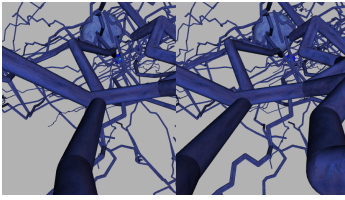


Figure 1: Left and right images for stereo vision and stressed perspective.

2.2. Camera Control

In complex scenes, the location of the user's viewpoint and the viewing direction can largely affect visibility. An intuitive camera control helps the user navigate along the virtual

world. To centralize the management of navigation in a single hand, the haptic device is used for controlling both the probe position and the camera, as suggested by [BC].

During navigation, a user can perform either probe translation actions or three types of camera and workspace transformation actions: (i) virtual workspace translations, (ii) virtual workspace rotations, and (iii) virtual workspace area zooming. All of them are controlled using a stylus-type haptic device.

The workspace area zooming and the virtual workspace rotation are haptically invariant. This means that those transformations do not change haptic feedback unless the probe changes its position. Virtual workspace translations are not haptically invariant because they entail a probe translation. It must be remarked that all virtual workspace transformations imply a camera motion to maintain the relative transformation between camera and probe. This makes the control of the haptic device more intuitive, because its real-world direction of motion is consistent with the virtual-world direction of motion. The following expression defines the matrix \mathbf{T}_h that transforms the haptic probe from real-world coordinates to virtual-world coordinates in pre-multiplication order $\mathbf{T}_h = \mathbf{T}_c \mathbf{R}_c \mathbf{S}_c \mathbf{T}_n$. \mathbf{T}_n normalizes the real-world haptic workspace and it depends on the manufacturer's specifications. \mathbf{T}_c , \mathbf{R}_c and \mathbf{S}_c are respectively a translation matrix, a rotation matrix, and a scale matrix, all of them defined based on camera properties. $\mathbf{T}_c = \mathbf{T}(\mathbf{c}_{pos})\mathbf{T}(-\mathbf{R}_c \mathbf{c}_{focal} \mathbf{v}_z)$ and $\mathbf{S}_c = \frac{1}{2} c_{focal} \tan(c_{angle}) \mathbf{I}$ assuming that, in the initial configuration, the camera points in the negative z-axis direction and its up vector points in the y-axis direction. c_{focal} is the focal distance, c_{angle} is the camera aperture angle, \mathbf{I} is the identity matrix, \mathbf{c}_{pos} is the camera position, \mathbf{v}_z is a unit vector in the z-axis direction, and $\mathbf{T}(\mathbf{v})$ defines a translation by a vector \mathbf{v} .

The gimbal rotations of the haptic device are transformed into rotations of the virtual workspace in the three axes. However, in practice, we use only the y-axis rotation, because the other two rotations were found to be unintuitive during preliminary testing. The haptic probe is used as the center of rotation to keep haptic feedback invariant. Workspace rotations imply the redefinition of two camera parameters: the current camera position $\mathbf{c}_{pos,n}$, and the current camera rotation $\mathbf{R}_{c,n-1}$. The rotation matrix $\mathbf{R}_{c,n}$ at the iteration n is defined by the expression $\mathbf{R}_{c,n} = \mathbf{R}_{c,n-1} \mathbf{R}(\mathbf{v}_y, \hat{a}_y) \mathbf{R}(\mathbf{v}_x, \hat{a}_x) \mathbf{R}(\mathbf{v}_z, \hat{a}_z)$ where $\mathbf{R}(\mathbf{v}, a)$ is the rotation matrix defined by the axis \mathbf{v} and the angle a ; \mathbf{v}_x , \mathbf{v}_y and \mathbf{v}_z are respectively the x-axis, y-axis and z-axis; and \hat{a}_i is defined by the expression:

$$\hat{a}_i = \begin{cases} 0 & , \text{if } \|a_i\| < a_{t,i} \\ a_f(a_i - \frac{a_i}{\|a_i\|} a_{t,i}) & , \text{in other cases} \end{cases} \quad (1)$$

where $i \in \{x, y, z\}$ is one of the gimbal degrees of freedom, a_i is the gimbal rotation angle in the i-axis and $a_{t,i}$ and a_f

are parameters defined by the user. $a_{t,i}$ defines a threshold angle for the smallest allowed rotation. a_f defines the rotation velocity. Finally the camera position can be defined by the expression $\mathbf{c}_{\text{pos},n} = \mathbf{p} + \mathbf{R}_{\mathbf{c},n} \mathbf{R}_{\mathbf{c},n-1}^{-1} (\mathbf{c}_{\text{pos},n-1} - \mathbf{p})$ where \mathbf{p} is the current probe position.

Regarding scaling operations, we use the haptic device buttons to zoom in and out the scene. We use the position of the haptic probe as the center of the scaling to avoid sudden haptic force changes. We are determined the focal distance as $c_{focal,n} = s_f c_{focal,n-1}$ and camera position as $\mathbf{c}_{\text{pos},n} = s_f (\mathbf{c}_{\text{pos},n-1} - \mathbf{p}) + \mathbf{p}$, where s_j is a zooming velocity defined by the user.

Additionally, we separate the workspace into two regions: a *static* region in the center of the virtual workspace, and a *dynamic* region near the boundary (Fig. 2). If the proxy moves into the dynamic region, the workspace is translated to keep the proxy inside the static region. We adapt the velocity of the translation to the scale of the virtual workspace. $\mathbf{c}_{\text{pos},n} = \mathbf{c}_{\text{pos},n-1} + \mathbf{v}$ where \mathbf{v} is the vector $\mathbf{v} = \{v_i | i \in \{x, y, z\}\}$:

$$v_i = \begin{cases} 0 & , \text{ if } \frac{\|p_i\|}{\mathbf{S}_{\mathbf{c}}(i,i)} > v_t \\ v_f \left(\frac{p_i}{\mathbf{S}_{\mathbf{c}}(i,i)} - \frac{p_i}{\|p_i\|} v_t \right) & , \text{ in other cases} \end{cases} \quad (2)$$

where $\mathbf{S}_{\mathbf{c}}(i,i)$ is the element i, i of the current scaling matrix $\mathbf{S}_{\mathbf{c}}$ and v_t and v_f are user defined parameters. v_t defines the static working area and v_f defines the translation velocity.

To avoid workspace limitations of the haptic device, we also allow the user to center the virtual workspace on the current position of the haptic probe. To do so, the two haptic device buttons have to be pressed simultaneously and the virtual workspace is moved smoothly to its new goal position.

2.3. Visual Aids

Different visual aids have been added. First, the virtual workspace is displayed as a wired box. If the users go outside this area, the camera will move with them. Second, another wired box shows the nominal workspace defined by the manufacturer to guarantee the quality of the haptic response (Fig. 2).

The haptic probe or some important branching node along the filiform path can be occluded by other structures. For this, when the user is getting close to a node, the directions of the node branches are displayed on the top right corner of the screen. A red arrow shows the branch where the proxy currently is (see Fig. 2, on the top-right).

Due to the size of neural structures, users typically operate on a small region of the scene. This makes them lose their sense of global position in the scene. We address this issue by displaying a small viewport with the location of the virtual workspace in the context of the complete scene.

2.4. Haptic Navigation

Understanding the visual representation of the neural filiform structures described in this paper can be difficult due to the tangled aspect of the image. We propose a natural way of using haptics to help in the data analysis. Our algorithm constrains the user's path to connected data elements, providing the user with the neural topology information through the haptic channel.

Our implementation lets the user disable and enable the haptic navigation mode. In free navigation mode, no haptic forces are rendered, and the user can move freely all along the data. In this mode, the haptic device is used only for camera control. In the constrained mode, we distinguish a proxy haptic position from the position of the actual haptic probe. The proxy is constrained to lie on the filiform neural structure at all times.

For constrained navigation, we represent a filiform structure as a set of nodes connected by linear segments. We denote as \mathbf{h} the (unconstrained) position of the haptic probe in the virtual workspace, and as \mathbf{p} the position of a proxy point that (locally) minimizes the distance to \mathbf{h} and is constrained to lie on the filiform structure. For visual feedback, we display to the user the proxy as a small sphere. On each step of the haptic update loop, we compute the new position of the proxy, and a feedback force as $\mathbf{f} = K(\mathbf{p} - \mathbf{h})$ where K is a stiffness constant that can be defined by the user. The force is transformed from the virtual workspace to the device workspace, and then it is displayed to the user with a haptic device. The force is transformed to be consistent with camera transformations.

To capture the user's intended motion, we propose a search algorithm that travels along the filiform structure by reducing the distance to the haptic probe, i.e. following a path of negative distance gradient. The navigation approach can thus be regarded as a gradient-descent optimization approach.

3. Results

We have tested our navigation system on multiple neural datasets (synthetic and neural data extracted from real segmented information [NMO]) (Fig. 2). Several volunteers (computer scientists with previous experience with haptic devices, as well as neurobiologists) have tested the system (Fig. 3). Subjects were instructed to navigate along the various synthetic and real datasets consisting of filiform structures. The navigation system performed interactively on all the datasets shown.

Preliminary perceptual experiments were performed with ten computer scientists (seven men and three women). They tested two datasets (Fig. 2). In both of them, a filiform structure highlighted in red indicated the path to be traversed along the axons. The users were instructed to evaluate two

aspects: camera control and the constrained navigation technique. Users rated whether the camera control was intuitive following a Likert scale, taking the maximum and minimum values as a very intuitive and as little intuitive control, respectively. 80% of them indicated that the camera control was intuitive. For the constrained navigation technique, users rated its usability on a scale from one to five, and the average score was 3.95.

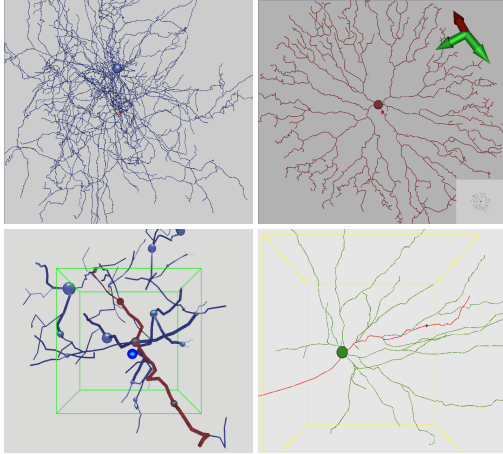


Figure 2: On the top, two brain datasets obtained from real data. On the bottom, the two datasets employed in the user studies.

Similar tests were conducted with several neurobiologists. They suggested that the tool is very useful to analyze and explore 3D models of large neuronal columns. According to their comments, haptic guidance along neural segments helped them to reach faster their points of interest. We also found that neurobiologists made fewer mistakes when the stereo module was active.



Figure 3: Image of a person testing our system

4. Conclusions and Future Work

The large complexity of the neural system in the human brain makes its understanding very hard using standard visualization approaches. Our experiments indicate that enhancing the visualization with a stereo system, intuitive camera control, and visual aids helps users get a better sense of the neural structure. Moreover, the addition of a haptically constrained navigation system allows users to follow specific

real neural structures and analyze them faster and in greater detail.

Several preliminary tests indicate that our navigation system is intuitive and easy to handle. Some neurobiologists have already expressed interest in using our multimodal interface to analyze their data in their daily work.

We are currently working to include guided navigation solutions that could attract users to specific points of interest. From an algorithmic point of view, the key problem to address is the intuitive combination of guiding forces and navigation feedback forces. We also consider extending our current navigation system with augmented reality solutions, even giving users the possibility to take notes dynamically over the data.

Acknowledgements

This work has been partially funded by the Spanish Ministry of Science and Innovation (grants TIN2007-67188, TIN2009-07942, TIN2010-21289 and the Cajal Blue Brain Project).

References

- [BC] BOECK J. D., CONINX K.: Haptic camera manipulation: Extending the camera in hand metaphor. In *Proceedings of Eurohaptics 2002*, pp. 36–40. 2
- [BOYBK] BROOKS F. J., OUH-YOUNG M., BATTER J., KILPATRICK P. J.: Project grope: Haptic displays for scientific visualization. In *Proceedings of SIGGRAPH 90*, vol. 24. 1
- [GL09] GAO Z., LECUYER A.: Path-planning and manipulation of nanotubes using visual and haptic guidance. In *Proceedings of IEEE International Conference on Virtual Environments Human-Computer Interfaces and Measurement Systems (2009)*, vol. 1, pp. 1–5. 1
- [KK10] KAMATH R., KAMAT R.: An effective stereo visualization system implementation for virtual prototyping. *International Journal on Computer Science and Engineering* (2010). 1
- [KRH*06] KLEIN J., RITTER F., HAHN H. K., REXILIUS J., PEITGEN H.-O.: Brain structure visualization using spectral fiber clustering. In *Proceedings of ACM SIGGRAPH 2006 Research posters* (2006), p. 168. 1
- [LHH*] LASSERRE S., HERNANDO J., HILL S., SCHÜERMANN F., JAOUDE G. A., DE MIGUEL P., MARKRAM H.: A neuron membrane mesh representation for visualization of electrophysiological simulations. *IEEE Transactions on Visualization and Computer Graphics*. In press. 1
- [Mar06] MARKRAM H.: The blue brain project. *Nat Rev Neurosci* (2006), 153–160. 1
- [MMYK06] MELEK Z., MAYERICH D., YUKSEL C., KEYSER J.: Visualization of fibrous and thread-like data. In *Visualization and Computer Graphics, IEEE Transactions on* (2006), pp. 1165–1172. 1
- [NMO] NeuroMorpho.org <http://neuromorpho.org/neuroMorpho/>. 3
- [TKCM] TURRO N., KHATIB O., COSTE-MANIERE E.: Haptically augmented teleoperation. In *Proceedings of the 2001 IEEE International Conference on Robotics and Automation*, vol. 1, pp. 386–392. 1